Aluminum to copper thermal compression bonding for heterogeneous integration of legacy dielets

Krutikesh Sahoo
UCLA Center for Heterogeneous Integration and Performance Scaling
Los Angeles, US
krutikesh@ucla.edu

Vineeth Harish
UCLA Center for Heterogeneous Integration and Performance Scaling
Los Angeles, US
vineeth@ucla.edu

Jui-Han Liu
UCLA Center for Heterogeneous Integration and Performance Scaling
Los Angeles, US
jhliu10@ucla.edu

Randall Irwin
UCLA Center for Heterogeneous Integration and Performance Scaling
Los Angeles, US
rirwin004@ucla.edu

Cheng-Ting Michael Yang
UCLA Center for Heterogeneous Integration and Performance Scaling
Los Angeles, US
ctyang@ucla.edu

Henry Sun
UCLA Center for Heterogeneous Integration and Performance Scaling
Los Angeles, US
hsunhenry@ucla.edu

Subramanian S. Iyer
UCLA Center for Heterogeneous Integration and Performance Scaling
Los Angeles, US
s.s.iyer@ucla.edu

2024 IEEE 74th Electronic Components and Technology Conference (ECTC) | 979-8-3503-7598-5/24/$31.00 ©2024 IEEE | DOI: 10.1109/ECTC51529.2024.00329

***Abstract*— Advanced packaging aims to integrate multiple heterogeneous chiplets/dielets at fine (≤ 10 µm) bonding pitches, irrespective of their size, material and function. Metal-to-metal thermal compression bonding (TCB) using copper-copper (Cu), gold-gold (Au), copper-gold interconnects is a versatile technique to reduce die-to-wafer bonding pitches up to 5 µm. However, a scalable metal-to-aluminum (Al) thermal compression bonding process does not currently exist, and all aluminum terminated dielets from the foundry are integrated using conventional solder-based processes, which limits their pitch scaling to 20µm. In this work, we develop an aluminum-to-copper thermal compression bonding process based on a two-step bonding approach, accompanied by hydrofluoric acid and in-situ formic acid vapor treatments to enable solderless Al-Cu bonding. An optimized Al-Cu bonding process will enable integration of Al-terminated legacy dielets and Cu-terminated advanced dielets on the same Si-based packaging substrate such as the silicon interconnect fabric (Si-IF), eliminating the need for solder bumping for legacy Al-terminated dielets. In this paper, bonding challenges to aluminum, the impact of surface treatment and annealing on Al-Cu interface, and results on shear strength and electrical daisy chain measurements are included. The calculated specific contact resistance of Al-Cu contacts is found to be 0.838 Ω·µm². Furthermore, we have also implemented, for the first time, a heterogeneous assembly consisting of Al-Cu TCB, Cu-Cu TCB and Au-Cu TCB on the same Si-IF silicon substrate.**

Keywords—thermal compression bonding, silicon interconnect fabric, aluminum, copper, advanced packaging, heterogeneous integration

I. Introduction

As heterogeneous integration of dielets becomes more ubiquitous, a diversity of dielets will need to be integrated on advanced packaging substrates. Solderless metal-metal thermal compression bonding (TCB) [1] provides a versatile assembly platform and previously we have shown TCB of Gold-Gold (Au) [2], Gold-Copper (Cu) [3], Copper-Copper [4, 15] etc. with appropriate interlayers. However, Aluminum (Al) terminations are difficult to work with, because of the almost immediate uniform and self-limiting oxidation of the surface – which is very difficult to penetrate. Nonetheless, many legacy technologies use Al as their last metal layer, either to provide compatibility with solder bumping, or in the case of analog and mixed signal chips, as a thick low conductivity metallization and routing layer for inductors and such. Thus, the use of Aluminum in the last metal layer is to achieve a lot more than just acting as a termination pad. One such example of a stack terminating in Al pads is the is shown in Fig. 1. Developing a TCB process to bond Cu pillars to Al pads is an important step in integrating these legacy dielets directly onto advanced packaging substrates with Cu termination. In this work, we propose a novel two-step Al-Cu bonding process to integrate such legacy dielets (which

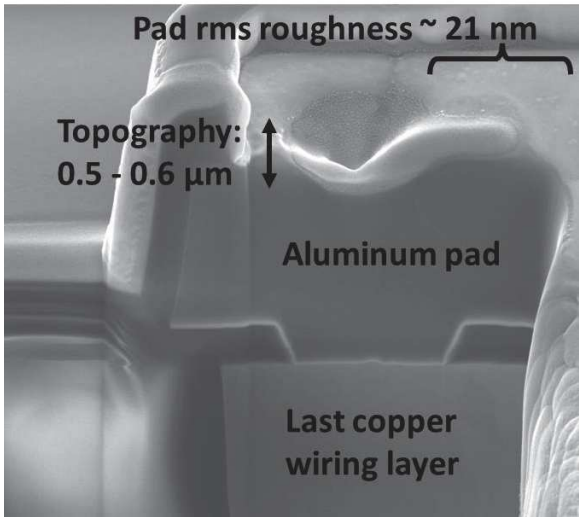

Fig. 1 A standard metal stack option in 22 nm fully depleted silicon on insulator (22FDX) dielet from GlobalFoundries which shows termination with aluminum (Al) pads. The measured rms pad roughness is ~ 21 nm and a topography of 0.5 - 0.6 µm is observed due to Al being deposited instead of following a damascene flow like copper.

2377-5726/24/$31.00 ©2024 IEEE
DOI 10.1109/ECTC51529.2024.00329

terminated with Al pads) on the Silicon Interconnect Fabric (Si-IF) [1 – 5, 15] and similar Si-based substrates. This will allow Si-IF and other Si-based platforms, to integrate both legacy and state-of-the-art dielets (in which dielets are terminated with Cu pads for TCB or hybrid bonding) on the same substrate without the need for additional packaging layers such as interposers, silicon-bridges, laminates etc. or need for a hybrid solder plus copper pillar process on the same substrate, which can be difficult to develop.

However, there are several challenges in developing an Al-Cu TCB process to work in air or nitrogen-rich environment which is available in current die-to-wafer bonding tools. Most notable is the fact that metallic Al is highly reactive with atmospheric oxygen, and it will form aluminum oxide (Al_2O_3) of ~ 5 nm thickness within a few milliseconds of being exposed to air [6]. This Al_2O_3 is a good diffusion barrier [8] and will prevent any interdiffusion during bonding and needs to be removed prior to bonding. Secondly, Al, which is used as a terminal metal layer in foundry process does not use a damascene flow and tends to be deposited. This results in a higher roughness when compared to the damascene process and topography as seen in Fig. 1 which needs to be addressed. Thirdly in a dissimilar system like Al-Cu, there is intermetallic formation at the joint contours [7] which can lead to reliability challenges. We expect that reliability can be improved by passivating any exposed Cu on pillars as well as the bonding interface using atomic layer deposition of alumina as described in our previous work [8]. In this work, we aim to develop an Al-Cu TCB process by overcoming such challenges. This paper is organized as follows: Section II of the paper summarizes the previous works done to enable bonding to Al pads, section III represents our experimental approach, section IV shows our results and inferences, and section V concludes the paper.

II. Background on Aluminum Bonding

In our survey of literature, we did not find significant progress on Al-Cu bonding, although several works [10 – 12] have demonstrated Al-Al bonding in both die-to-wafer and wafer-to-wafer formats. As discussed earlier, one of the major challenges in bonding Al to itself or other metals is the native oxide layer of Al_2O_3, which, while easily removed using wet or atomic layer etching techniques [9], rebuilds almost instantly when sample is exposed to air. So far one of the successful ways to remove this oxide is to do argon treatment under vacuum. A collective die-to-wafer bonding was recently demonstrated by Schulze et al. [10] in a vacuum environment with an argon in-situ clean to remove the native oxide. Dies with aluminum pads were placed in pockets on a silicon wafer and bonded to another wafer with aluminum pads at 300°C with pressures between 52 and 60 MPa. The resulting resistance per contact of 32.3 mΩ indicated successful bonding. In another study, wafer-to-wafer Al-Al bonding was conducted with the same in-situ Argon pre-treatment under vacuum. The results showed successful bonding at pressures less than 2 MPa at temperatures less than 150°C [11]. This study indicated aluminum will naturally bond to aluminum if the oxide is removed at low pressure and temperature. This observation was also explored in a study by CEA-LETI [12] for room temperature die to wafer Al-Al cold bonding. In this study, aluminum coated micro-tubes made of tungsten silicide (WSi) were used to plastically deform an aluminum pad such that the micro-tube would pierce the aluminum oxide layer and form a metallic bond between the Al layer on the micro-tube and the oxide free Aluminum in the bulk of the pad. Successful bonding was achieved across 100,000 connections by applying 8mN per connection. However, when applied to a dielet with active devices, such force per dielet has a possibility of damaging the active devices leading to circuit failures.

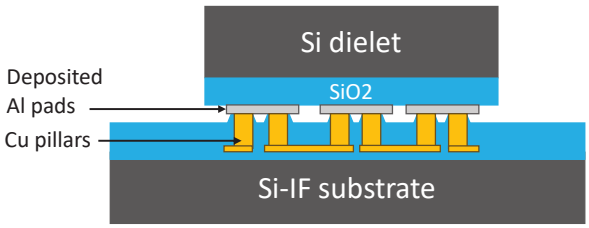

Fig. 2 The schematic of the samples used for optimization of the aluminum-copper thermal compression bonding (TCB) process.

This work explores the bonding mechanism between Al and Cu. The importance of Al-Cu TCB has already been established in section I. The next section describes in detail the experimental approach taken including sample preparation, surface pre-treatment, bonding procedure, and analysis techniques.

III. Experimental Approach

To develop the aluminum-copper die-to-substrate bonding process in ambient air, dielets with aluminum (Al) pads and substrate with copper (Cu) pillars were fabricated. The Al was deposited by dc sputtering using an Al 99.5% Cu 0.5% target. The Al sputtering was done on thermally grown silicon dioxide (SiO_2) and then the film patterned to create Al pads on dielets. The thickness of deposited Al pads was 500 nm. Fig. 2 shows the schematic of the sample used for bonding and testing. On the substrate side, a single Cu damascene process is used to fabricate Cu pillars of 5µm diameter and 10µm pitch as described in our previous work [4].

As discussed in Section II, surface pretreatment prior to bonding is essential to allow Aluminum and Copper inter-diffusion during bonding. Copper oxide can be removed by in-situ clean with formic acid vapor as described in our previous works [3, 4, 15]. Removing aluminum oxide, however, poses challenges. Since the dielet tacking process is to operate in air, standard argon treatment described in section II will not be feasible, as even with argon treatment prior to bonding, Al will re-oxidize as soon as it is exposed to air. Also, the formic acid vapor technique which can clean copper oxide proved ineffective to clean Al_2O_3 in our initial bonding tests. Therefore, the surface treatment was planned with the goal of temporarily converting Al_2O_3 into another film which would be easy to decompose during bonding. Aluminum Fluoride ($AlF_3.xH_2O$) is found to be a suitable candidate due to its low solubility in acids, bases and water [14] when compared to other salts of Al. As shown in Fig. 3, several treatments were used to synthesize aluminum fluoride on Al pads, however a 3 second dip in diluted hydrofluoric (HF) acid (ratio 1:10) proved to be the best approach. Energy dispersive spectroscopy (EDS) was used to

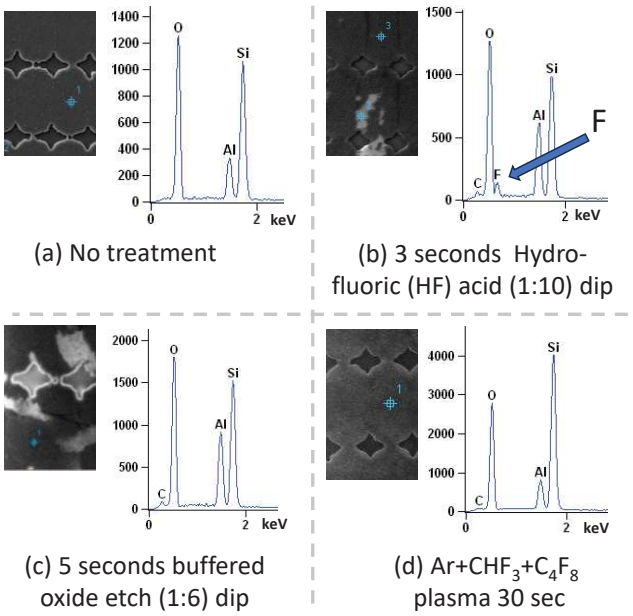

Fig. 3 Surface treatment done on Aluminum pads prior to bonding. The goal of the surface treatment is to remove aluminum oxide from the pads and deposit aluminum fluoride. (a) shows control sample, (b) shows surface treatment using dilute hydrofluoric acid (HF) where we can see a fluorine peak in the energy dispersive spectroscopy (EDS). (c) shows surface treatment with buffered oxide etch (BOE) 1:6 solution. (d) shows surface treatment in argon and fluorine plasma. In (c) and (d) no fluorine peak is observed.

verify the existence of fluorine peak, which was visible in samples treated with dilute HF. This is shown in Fig. 3(b). Longer exposure to HF lead to the etching of Al pads.

The bonding process is a high throughput (> 1000 units per hour) dielet tack and anneal process demonstrated in our previous work [15]. The first step in the bonding process is a 10 second tacking process for dielet-attach. This is followed by a batch annealing process for metal-to-metal diffusion and grain growth. The two steps are schematically represented in Fig. 4. The bonding parameters used are given in Table 1.

The bonding quality is determined by a die-shear test performed using Nordson Dage equipment [16]. In addition, energy dispersive X-ray spectroscopy (EDS) was extensively used for material surface analysis, and investigation of Al-Cu joints post annealing. This would be important to determine the condition of Al surface after surface treatments and to determine whether diffusion occurs between Cu and Al during the bonding process. Al-Cu Adhesion was further verified using Crosshatch adhesion tape testing. Finally, four probe resistance measurements using daisy chains were used for contact resistance calculations.

IV. Results and Discussion

Fig. 4(d). shows an example of a several assemblies bonded using Al-Cu two-step TCB. Post bonding, dielets were sheared to measure bonding quality using shear force. The average shear force across 20 samples was found to be 13 N though the maximum shear force was observed to be 40.12 N. For a 2×2

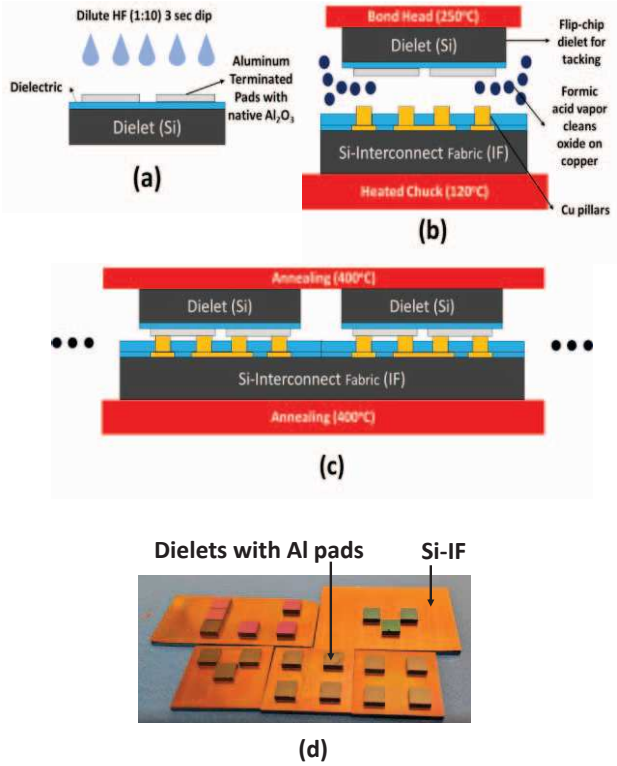

Fig. 4 A two-step approach for Al-Cu bonding. The two-step approach comprises of die tacking and annealing and is described in detail in [15]. (a) presents the surface treatment on dies, (b) represents dielet tacking with in-situ formic acid vapor cleaning, (c) represents annealing of several dies after assembly. (d) shows several samples prepared using two step TCB which are used for shear and electrical measurements.

mm^2 dielet to pass military standard (MIL-SPEC 883) [17] shear strength specification, the minimum expected shear force is 25 N. Therefore, the measured average shear was found to be below the minimum requirement. The sheared dielets and substrates were investigated further to find the reason behind large variation in shear strength.

TABLE I. Parameters chosen from [15] for Al-Cu TCB

Parameter name	*Value*	*Unit*
Die cleaning time	5	s
Die placement time	3	s
Chuck temperature	120	ºC
Tacking pressure	250	MPa
Annealing temperature	400	ºC
Annealing pressure	150	MPa

A. EDS analysis of the sheared dielet and Si-IF pillars.

The sheared die and substrate were analyzed using energy dispersive X-ray spectroscopy (EDS). Fig. 5 shows the Al pads under the dielet after shearing, both visually as well as under

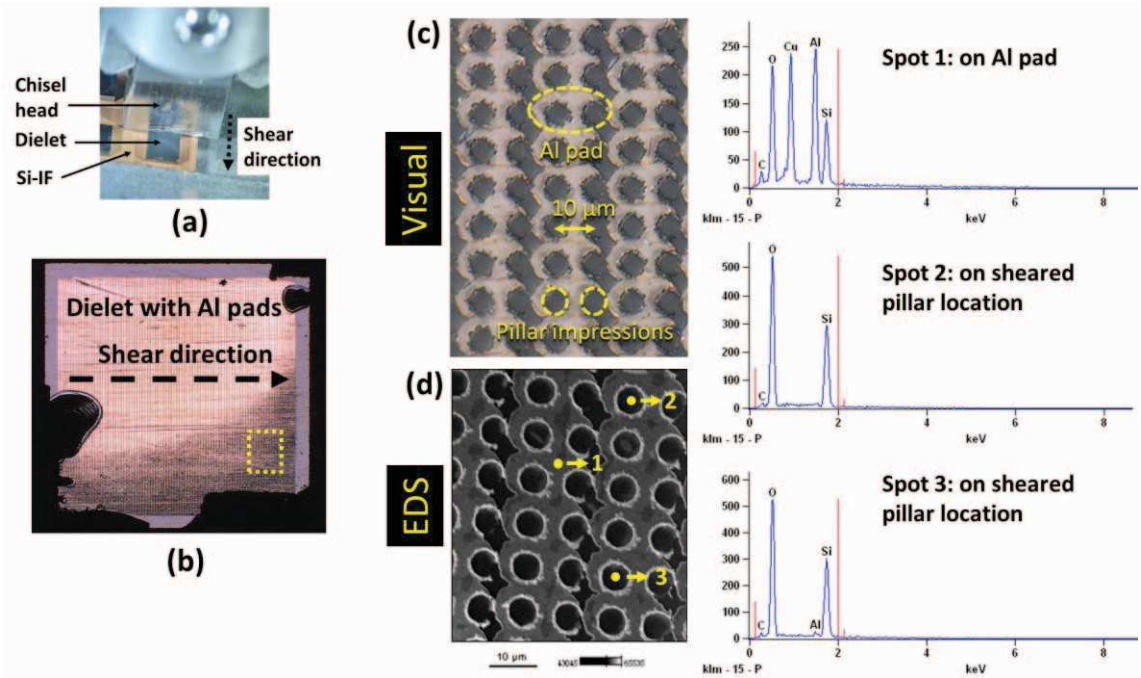

Fig. 5 (a) Setup for dielet shear using Nordson Dage equipment (b) sheared dielet with Al pads. The dashed yellow box is enlarged for visual inspection and energy dispersive spectroscopy (EDS) analysis. (c) visual inspection of Al pads on dielet. After fabrication it was found out that Al pads were shorted and hence these samples were only used for mechanical analysis and not electrical analysis. (d) EDS spectra at three spots on the sample. Spot 1 is on an Al pad, spot 2 and spot 3 is on positions from where Cu pillar was sheared during the dielet-shear test.

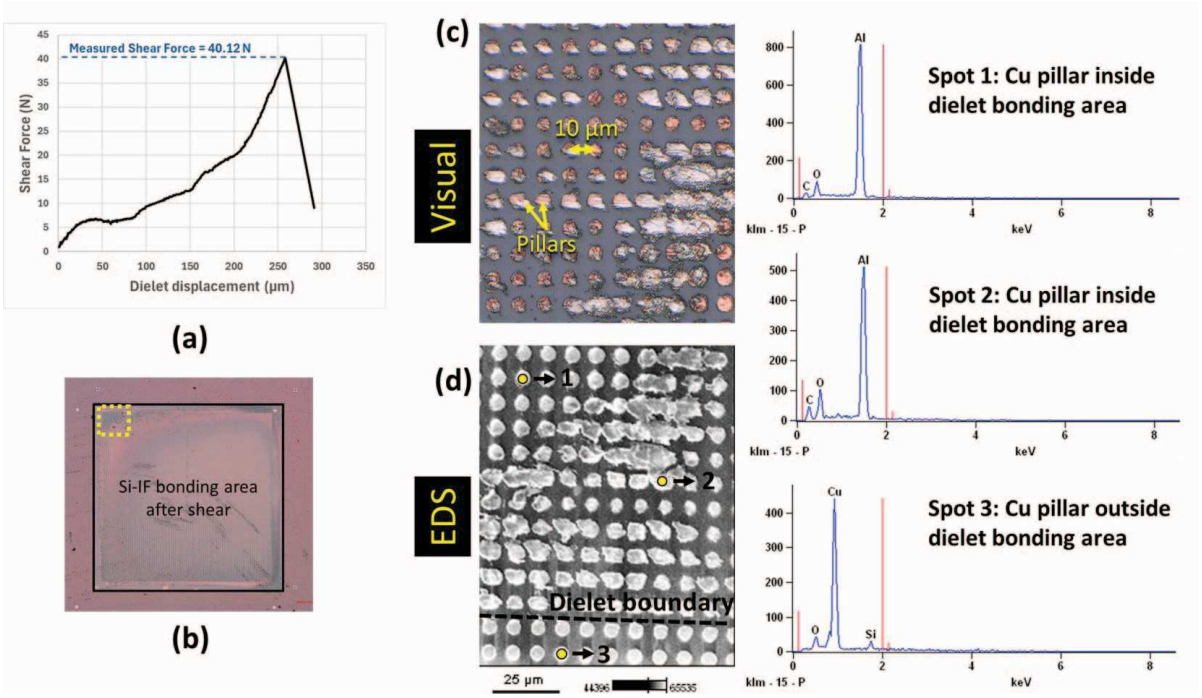

Fig. 6 (a) Force vs. displacement curve for shear measurement showing a maximum shear force of 40.12 N (b) sheared Si-IF with Cu pillars. The dashed yellow box is enlarged for visual inspection and energy dispersive spectroscopy (EDS) analysis. (c) visual inspection of Cu pillars which shows that Al is transferred to the Cu pillars after shear. (d) EDS spectra at three spots on the Si-IF sample. Spot 1 and spot 2 are on Al covered Cu pillars within the bonding area. Spot 3 is on a Cu pillar outside the bonding area.

EDS. The patterned circles within each Al pad are the locations where Cu pillars were bonded to Al before being sheared off. Three spots were chosen for EDS analysis. Spot 1 is on an Al pad, therefore material analysis at spot 1 reveals a strong peak for Al. A strong peak for Cu is also observed at spot 1 as the target used to sputter Al has 0.5% Cu. Next, we observe spots

2 and 3. Elemental analysis at spot 2 reveals no Al signal or Cu signal. A similar result is observed at spot 3 with a negligible Al signal. These are the places where Cu pillars got sheared off during the dielet-shear process. The results indicate that after anneal, the Al has completely delaminated from the Al pads at the areas where it contacted the Cu pillar during bonding. Naturally, we next perform EDS of pillar side on Si-IF to figure out if Al has transferred to the Cu pillars.

As seen in Fig. 6, EDS analysis was done on the Cu pillars on the Si-IF side post bonding and dielet shear. Al can be visually seen on Cu Pillars in Fig. 6 (c) which can be confirmed through EDS. Again, three spots were chosen for material analysis. In the EDS micrograph, a dashed line divides the dielet bonding region such that Cu pillars above the dashed line are in the bonding region while Cu pillars below the dashed line are outside the bonding region. Spots 1 and 2 are on Cu pillars within the bonding region and a strong Al peak can be observed on both pillars indicating detection of Al on Cu pillars. Spot 2 is outside the bonding region, and we can see only the Cu peak on Cu pillars which is to be expected as no bonding is taking place at this location. A small oxygen peak is also observed indicating oxidation of the assembly during sample preparation for characterization. This can be reduced or eliminated by passivating the assembly using atomic layer deposition of alumina as described in [8].

B. Adhesion test of Aluminum on Copper pillars

While EDS inspection indicates the presence of Al on Cu pillars, it does not guarantee any adhesion or diffusion between them. It is entirely possible while shearing, the aluminum pads get detached from the dielet and are attached to Cu pillars through weak Van der Waal's forces. To confirm whether Al is bonded to Cu on the pillars, we subject the samples to cross-hatch adhesion tape test. The tape used is a model of 600-1PK produced by 3M company in America [18]. The testing is performed by a tester designed according to the standard of ISO2409-192. The adhesion tape is applied to the Si-IF which has Al on Cu pillars. The results after tape test are observed at two regions 1 and 2 as seen in Fig. 7 (a). Fig. 7 (b) shows the condition of the surface before and after tape test in region 1 and region 2. In both the cases, Al still exists on Cu pillars after tape tests, indicating good adhesion. We have also confirmed the same through EDS analysis. The tape test was repeated multiple times without any further Al removal from Cu pads.

It should be noted that at the center of the dielet to substrate assembly, significant Al was not observed on the Cu pillars indicating poor dielet attach at the center. We predict lower bonding pressure at the dielet center compared to dielet edge to be a cause of this. Further optimization of Al-Cu thermal compression bonding is required to improve bonding strength.

C. Discussion of the results

After the observations from EDS as well as from adhesion tape test, we infer that a large variation in shear force leading to an average shear force of ~13 N could be due to the following reasons:

- To recall, the dielets with Al pads were fabricated by sputtering Al on SiO2 dielectric. At room temperature the adhesion of Al to SiO2 is confirmed by tape test, however after undergoing thermal cycling in the annealing chamber, due to significant differences in coefficient of thermal expansion i.e. CTE of Al (21 - 24 ppm/^{o}C [19]) and CTE of SiO_2 (0.55 - 0.75 ppm/^{o}C [20]) there could be weakening of the adhesion between Al and SiO2. This could lead to a premature detach of Al and SiO_2 during die-shear test on the Nordson Dage tool, which is also indicated by the EDS analysis at spot 2 and spot 3 on the dielet side as reported in Fig. 5. Under this condition, we do not actually measure the shear strength of Al to Cu, rather, the adhesion strength of Al to SiO_2. We expect the Al-Cu shear strength to be higher.

- The surface treatment done on Al pads may not be sufficient to keep the Al pads from oxidizing long enough for acceptable inter-diffusion between Al and Cu. We have also observed that at the center of the dielet, the Al transfer to Cu pillars is less than at the edge. These limitations can be overcome with better surface treatment optimization, or by using a die-to-wafer bonding chamber with vacuum or nitrogen ambient. However our goal has been to achieve aluminum to copper bonding in the air, which reduces necessity for new equipment development, and overall results in a less expensive process.

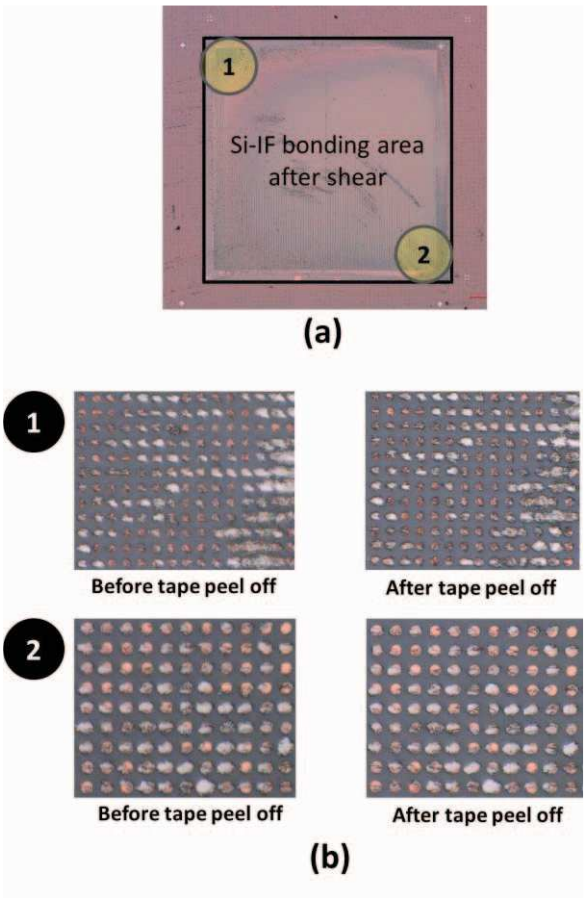

Fig. 7 (a) two locations on the Si-IF substrate where adhesion test was performed. (b) the results of the cross hatch adhesion test at location 1 and 2.

D. *Overcoming topography of Al pads in foundry dielets.*

As seen in Fig. 1, there is a topography of 0.5 – 0.6 µm on a foundry dielet which needs to be addressed. We do not expect this to be a challenge in case of legacy dielets which have large pads at pitch of 30µm and above as there is ample space for multiple Cu pillars at 10µm or below pitch to bond to these pads. However, if the bonding pad size is similar to pillar pitch, the topography can become a significant challenge. In this case, the height of the Cu pillars needs to be modified to accommodate the topography during bonding. For example, pillars of height 5 µm can be used to overcome topography of 0.5 – 0.6 µm on deposited Al pads. However, there could be processing and design limitations to increasing pillar heights and the relation between pad topography and pillar heights needs to be studied.

E. *Heterogeneous assembly and electrical measurements*

In our previous works, we have developed bonding process for copper-copper TCB [4, 15] as well as for gold-copper TCB [3]. Using this knowledge, a 2×2 heterogeneous assembly comprising of dielets having aluminum pads, copper pads and gold pads was successfully bonded to the same Si-IF substrate by using Al-Cu TCB, Cu-Cu TCB and Au-Cu TCB respectively. This is shown in Fig. 8 (a), and to our knowledge, it is the first ever demonstration of three types of bonding (Al-Cu, Cu-Cu and Au-Cu) on a single Si-based packaging substrate. Hence, we believe that thermal compression bonding can be used to assemble composite/heterogeneous assemblies comprising of III-V dielets which usually terminate in gold pads, advanced node foundry dielets (designed for hybrid bonding) which can terminate in copper pads and legacy node foundry dielets which usually terminate in aluminum pads on a single packaging substrate level.

Across the top two dielets of the 2×2 assembly, out of which one is a dielet with Al pads and another is a dielet with Cu pads, four probe daisy chain measurements were performed. All the 8 tested daisy chains were functional, and the current-voltage (IV) characteristics are presented in Fig. 8(c). However, it should be noted that there is significant variation in the resistance (up-to 5 Ω) of the links and the higher resistance links are found towards the center of the dielet. By performing a similar IV test on a separate Al-Cu bonded dielet, we have concluded the variation was due to Al-Cu bonding. This result, along with the low shear strength evaluation for Al-Cu bonding, mainly due to the reasons described in section IV(C) point to the fact that further improvement of Al-Cu bonding is necessary before reliable, large-scale assemblies can be built using Al-Cu TCB. After de-embedding the effects of measurement pads and resistance of Cu links, the Al-Cu specific contact resistance is found to be 0.838 Ω-µm^2. The overall results are encouraging. We believe further optimization of the surface treatment and annealing parameters is crucial to get reliable Al-Cu TCB and improve Al-Cu specific contact resistance.

V. Conclusion

In this work, we have shown our progress on aluminum-copper thermal compression bonding (Al-Cu TCB). We have shown Al-Cu bonding using necessary surface treatment is possible in air. We have also included electrical measurements for the bonded daisy chain links. While a few challenges related to shear strength and the scale-out of Al-Cu TCB to wafer-scale systems remain, we have a plan to overcome them. Al-Cu TCB significantly expands the capability and use-cases for thermal compression bonding. We believe the true potential of metal-metal direct thermal compression bonding can be realized by

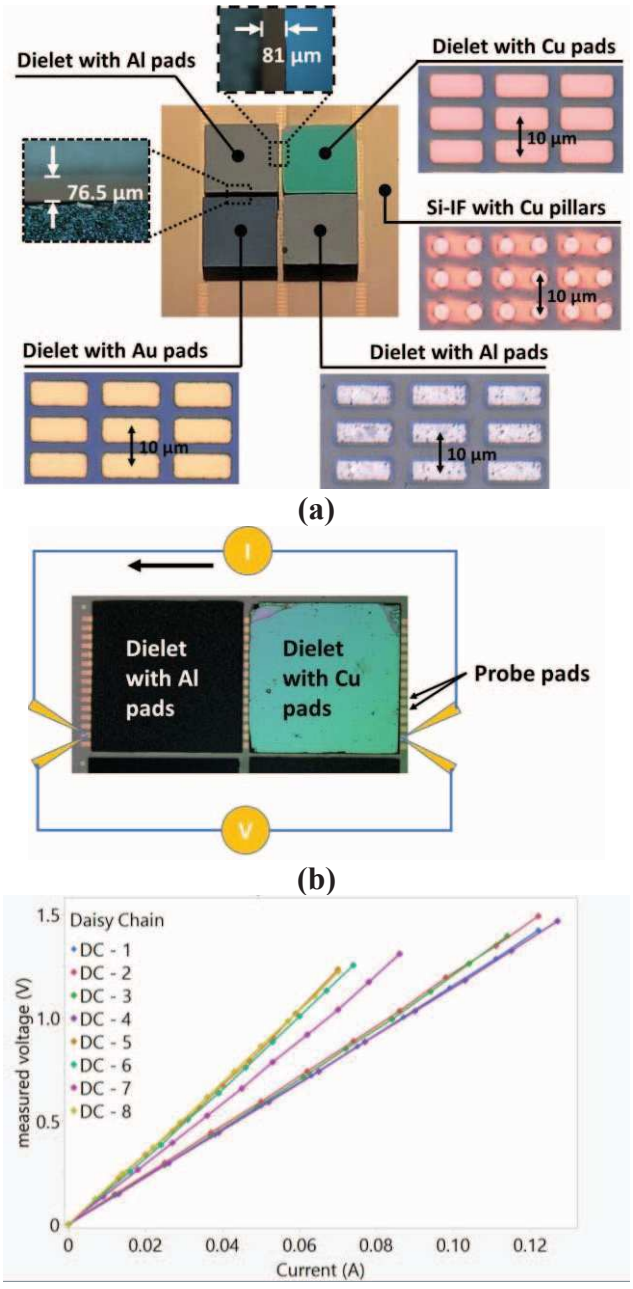

Fig. 8 (a) A 2×2 configuration sample with dielets bonded using Al-Cu TCB from this work and Cu-Cu TCB [4, 15] and Au-Cu TCB [3]. The inter-dielet spacing is < 100 µm. (b) four probe measurement setup across the top two dielets for electrical measurements (c) measurements across 8 daisy chains. Daisy chain resistance variation is attributed to die-to-wafer misalignment and further requirement for optimization of Al-Cu TCB.

developing processes for bonding dielets of different sizes as well as different materials (Cu-Cu, Au-Cu and Al-Cu TCB process), as shown in this work.

ACKNOWLEDGMENT

The authors would like to thank the UCLA CHIPS Consortium for their continued support. The authors would also like to acknowledge the facilities and staff of the UCLA Nanolab. Furthermore, this work was supported in part by CHIMES, one of the seven centers in JUMP 2.0, a Semiconductor Research Corporation (SRC) program sponsored by DARPA through the award S003591-SRC. The authors thank GlobalFoundries and Kulicke & Soffa for their support. The authors also thank Golam Sabbir, Haoxiang Ren, and Guangqi Ouyang for their valuable suggestions with writing of the paper.

REFERENCES

[1] S. S. Iyer, S. Jangam and B. Vaisband, "Silicon interconnect fabric: A versatile heterogeneous integration platform for AI systems," in *IBM Journal of Research and Development*, vol. 63, no. 6, pp. 5:1-5:16, 1 Nov.-Dec. 2019, doi: 10.1147/JRD.2019.2940427.

[2] A. A. Bajwa *et al*., "Heterogeneous Integration at Fine Pitch (≤ 10 µm) Using Thermal Compression Bonding," *2017 IEEE 67th Electronic Components and Technology Conference (ECTC)*, Orlando, FL, USA, 2017, pp. 1276-1284, doi: 10.1109/ECTC.2017.240.

[3] K. Sahoo, S. Pal, N. Shakoorzadeh, Y. -T. Yang and S. S. Iyer, "Copper to gold thermal compression bonding in heterogenous wafer-scale systems," *2021 IEEE 71st Electronic Components and Technology Conference (ECTC)*, San Diego, CA, USA, 2021, pp. 487-493, doi: 10.1109/ECTC32696.2021.00088.

[4] S. Jangam and S. S. Iyer, "Silicon-Interconnect Fabric for Fine-Pitch (≤10 μ m) Heterogeneous Integration," in IEEE Transactions on Components, Packaging and Manufacturing Technology, vol. 11, no. 5, pp. 727-738, May 2021, doi: 10.1109/TCPMT.2021.3075219.

[5] H. Ren, K. Sahoo, T. Xiang, G. Ouyang and S. S. Iyer, "Demonstration of a Power-efficient and Cost-effective Power Delivery Architecture for Heterogeneously Integrated Wafer-scale Systems," *2023 IEEE 73rd Electronic Components and Technology Conference (ECTC)*, Orlando, FL, USA, 2023, pp. 1614-1621, doi: 10.1109/ECTC51909.2023.00274.

[6] Luiz Fernando Mafra Mendes Freitas Santos, Felipe Chen Abrego, Katia Franklin Albertin Torres, Daniel Scodeler Raimundo, "Inducing aluminum oxide growth at room temperature and atmospheric pressure through low dose gamma-ray irradiation," Radiation Physics and Chemistry, Volume 204, 2023, 110666, ISSN 0969-806X, https://doi.org/10.1016/j.radphyschem.2022.110666.

[7] Hyoung-Joon Kim *et al*., "Effects of Cu/Al intermetallic compound (IMC) on copper wire and aluminum pad bondability," in *IEEE Transactions on Components and Packaging Technologies*, vol. 26, no. 2, pp. 367-374, June 2003, doi: 10.1109/TCAPT.2003.815121.

[8] N. Shakoorzadeh Chase, K. Sahoo, Y. Tao Yang and S. S. Iyer, "Atomic Layer Deposited Al2O3 Encapsulation for the Silicon Interconnect Fabric," 2020 IEEE 70th Electronic Components and Technology Conference (ECTC), Orlando, FL, USA, 2020, pp. 1241-1246, doi: 10.1109/ECTC32862.2020.00198.

[9] Firek, P., Szmidt, J., Nowakowska-Langier, K. and Zdunek, K., Electric Characterization and Selective Etching of Aluminum Oxide. Plasma Processes Polym., 6: S840-S843. https://doi.org/10.1002/ppap.200932103

[10] S. Schulze, T. Voß, P. Krüger and M. Wietstruck, "A collective die to wafer bonding approach based on surface-activated aluminum-aluminum thermocompression bonding," in *IEEE Transactions on Components, Packaging and Manufacturing Technology*, doi: 10.1109/TCPMT.2024.3363236.

[11] Bernhard Rebhan, Andreas Hinterreiter, Nishant Malik, Kari Schjølberg-Henriksen, Viorel Dragoi and Kurt Hingerl "Low-Temperature Aluminum-Aluminum Wafer Bonding, " 2016 ECS Transactions 75 15, doi: 10.1149/07509.0015ecst

[12] F. Marion *et al*., "Aluminum to Aluminum bonding at room temperature," *2013 IEEE 63rd Electronic Components and Technology Conference*, Las Vegas, NV, USA, 2013, pp. 146-153, doi: 10.1109/ECTC.2013.6575565.

[13] K. Sahoo, U. Rathore, S. Chandra Jangam, T. Nguyen, D. Markovic and S. S. Iyer, "Functional Demonstration of < 0.4-pJ/bit, 9.8 µm Fine-Pitch Dielet-to-Dielet Links for Advanced Packaging using Silicon Interconnect Fabric," *2022 IEEE 72nd Electronic Components and Technology Conference (ECTC)*, San Diego, CA, USA, 2022, pp. 2104-2110, doi: 10.1109/ECTC51906.2022.00332.

[14] Aluminum Fluoride synthesis information Available: https://www.scbt.com/p/aluminum-fluoride-7784-18-1

[15] K. Sahoo, H. Ren and S. S. Iyer, "A High Throughput Two-Stage Die-to-Wafer Thermal Compression Bonding Scheme for Heterogeneous Integration," *2023 IEEE 73rd Electronic Components and Technology Conference (ECTC)*, Orlando, FL, USA, 2023, pp. 362-366, doi: 10.1109/ECTC51909.2023.00067.

[16] Nordson DAGE 4000 plus bond tester, Available: https://www.nordson.com/en/products/test-and-inspection-products/dage-4000plus-bondtester

[17] MIL-SPEC 883, Available: https://s3vi.ndc.nasa.gov/ssri-kb/static/resources/std883.pdf

[18] 3M Science, Available: www.3m.com

[19] Thermal expansion coefficient of aluminum, available: https://www.engineeringtoolbox.com/linear-expansion-coefficients-d_95.html

[20] Thermal expansion coefficient of silicon dioxide, available: https://www.azom.com/properties.aspx?ArticleID=1114

[21] H. Ren *et al*., "Heterogeneous Power Delivery for Large Chiplet-based Systems using Integrated GaN/Si-Interconnect Fabric with sub-10 µm Bond Pitch," *2023 International Electron Devices Meeting (IEDM)*, San Francisco, CA, USA, 2023, pp. 1-4, doi: 10.1109/IEDM45741.2023.10413759.